JOURNAL OF NEUROTRAUMA 27:1283–1295 (July 2010)

DOI: 10.1089/neu.2009.1227

Minozac Treatment Prevents Increased Seizure Susceptibility in a Mouse "Two-Hit" Model of Closed Skull Traumatic Brain Injury and Electroconvulsive Shock-Induced Seizures

MaryAnn Chrzaszcz,[1,2] Charu Venkatesan,[1,2] Tina Dragisic,[1,2]
D. Martin Watterson,[3] and Mark S. Wainwright[1,2,3]

Abstract

The mechanisms linking traumatic brain injury (TBI) to post-traumatic epilepsy (PTE) are not known and no therapy for prevention of PTE is available. We used a mouse closed-skull midline impact model to test the hypotheses that TBI increases susceptibility to seizures in a "two-hit" injury model, and that suppression of cytokine upregulation after the first hit will attenuate the increased susceptibility to the second neurological insult. Adult male CD-1 mice underwent midline closed skull pneumatic impact. At 3 and 6 h after impact or sham procedure, the mice were injected IP with either Minozac (Mzc), a suppressor of proinflammatory cytokine upregulation, or vehicle (saline). On day 7 after sham operation or TBI, seizures were induced using electroconvulsive shock (ECS), and susceptibility to seizures was measured by the current required for seizure induction. Activation of glia, neuronal injury, and metallothionein-immunoreactive cells were quantified in the hippocampus by immunohistochemical methods. Neurobehavioral function over 14-day recovery was quantified using the Barnes maze. Following TBI there was a significant increase in susceptibility to seizures induced by ECS, and this susceptibility was prevented by suppression of cytokine upregulation with Mzc. Astrocyte activation, metallothionein expression, and neurobehavioral impairment were also increased in the two-hit group subjected to combined TBI and ECS. These enhanced responses in the two-hit group were also prevented by suppression of proinflammatory cytokine upregulation with Mzc. These data implicate glial activation in the mechanisms of epileptogenesis after TBI, and identify a potential therapeutic approach to attenuate the delayed neurological sequelae of TBI.

Key words: astrocyte; electroconvulsive shock; microglia; seizure; traumatic brain injury

Introduction

Post-traumatic epilepsy (PTE), cognitive impairment, and dementia are long-term medically intractable complications of TBI (Sosin et al., 1996; Waxweiler et al., 1995). More than 20% of adults have a spontaneous seizure within 2 years of TBI associated with intracranial hematoma, depressed skull fracture, cortical contusion, or penetration of the brain (Weiss et al., 1983). Prophylactic anticonvulsant therapy decreases the occurrence of seizures early after TBI during the first week after injury, but has no effect on the incidence of seizures occurring after more than 1 week of recovery (Teasell et al., 2007). Meta-analysis of the efficacy of anticonvulsants for seizure prevention suggests that they may increase the risk of seizures under some conditions (Temkin, 2001). The mechanisms responsible for PTE are not known.

Neuroinflammation is the term used to describe the CNS inflammatory responses produced by activated glia. Glial activation (astrocytes and microglia) occurs as a protective or pathological response to CNS insults (Perry et al., 2007). Uncontrolled glial activation may contribute to the progression of neurological disease, resulting in enhanced production of proinflammatory cytokines, including IL-1β, TNF-α, and S100B (Van Eldik and Wainwright, 2003; Wyss-Coray, 2006). Glial activation is a recognized response to seizures (Rizzi et al., 2003), and may contribute directly to mechanisms of

[1]Department of Pediatrics, Division of Neurology, [2]Center for Interdisciplinary Research in Pediatric Critical Illness and Injury, and [3]Center for Molecular Innovation and Drug Discovery, Northwestern University Feinberg School of Medicine, Chicago, Illinois.

epileptogenesis (Ravizza et al., 2005; Vezzani and Baram, 2007). Experimental and clinical evidence has identified inflammatory responses as a significant mechanism contributing to neurological dysfunction in head injury (Schmidt et al., 2005) and epilepsy (Vezzani and Granata, 2005). In a rat weight-drop (Golarai et al., 2001) and a controlled cortical impact (CCI) model (Statler et al., 2008), TBI lowered post-traumatic seizure thresholds. However, the contribution of activated glia to the reduction in the seizure threshold is not known.

In the present studies, we used a mouse closed-skull TBI model (Lloyd et al., 2008; Wang et al., 2007) to test the hypothesis that TBI results in increased susceptibility to seizures, and that this enhanced response to a seizure-inducing "second-hit" is due to an increase in activated astrocytes and microglia. To quantify changes in seizure threshold produced by TBI, and to deliver a controlled second-hit, we allowed mice to recover for 7 days before administering an electroconvulsive shock (ECS), a well-established method for seizure induction in the rodent (Ferraro et al., 2002; Frankel et al., 2001). As an initial step toward determining the mechanisms by which activated astrocytes affect neuronal function, we measured changes in the zinc binding protein metallothionein, which is released from astrocytes in response to neuronal injury (Chung et al., 2004). To determine whether the effects of TBI on seizure susceptibility were linked to activation of astrocytes or microglia, we measured changes in GFAP, S100B, and the microglial protein Iba1, and treated mice following TBI with the CNS-penetrant small molecule Minozac (Mzc). As we have previously reported, Mzc treatment suppresses proinflammatory cytokine upregulation resulting from TBI (Lloyd et al., 2008), or kainic acid–induced seizures (Somera-Molina et al., 2009).

We report here that TBI increases susceptibility to a second-hit of ECS-induced seizures after 7 days of recovery, resulting in a reduction in the threshold of ECS required to cause seizures. Mice subject to two hits also show greater neurobehavioral impairment than mice subject to TBI alone. Astrocyte and microglial activation was greater in the two-hit animals subjected to the combination of TBI and ECS. Notably, the reduced seizure threshold produced by TBI, and exaggerated neurobehavioral impairment seen in the two-hit mice, was prevented by suppression of glial activation by treatment with Mzc. These data support a role for activated astrocytes and microglia in the mechanisms behind epileptogenesis following TBI.

Methods

Animal care and housing

All experiments were performed in accordance with the National Institutes of Health Guide for Care and Use of Laboratory Animals. The Children's Memorial Research Center Institutional Animal Care and Use Committee approved all experimental procedures. Adult CD1 male mice weighing 20–25 g were used for these experiments.

Mouse model of closed head injury

Mice were subjected to closed-skull traumatic brain injury using a stereotactically guided pneumatic compression device with minor modification of published methods as previously described (Lloyd et al., 2008). Briefly, the mice were anesthetized with isoflurane (4% induction, 1.5% maintenance) in 100% oxygen. After endotracheal intubation, the mice were mechanically ventilated (Hugo Sachs Electronik, March-Hugstetten, Germany), using a protective ventilation strategy (3 cm H_2O positive end-expiratory pressure; tidal volume 5 mL/kg) as previously described (Wainwright et al., 2003). Core temperature was monitored using a rectal probe (IT-18; Physitemp, Clifton, NJ) and maintained at $37.0 \pm 0.1^{\circ}C$ by surface heating and cooling. The mice were secured in prone position in a customized resin mold. A midline sagittal scalp incision was made and the periosteum reflected to reveal the appropriate landmarks. A concave 3-mm metallic disk was affixed in the midline, immediately caudal to the bregma at -0.10 mm. A midline closed skull impact was delivered using a pneumatic impactor (Air-Power Inc., High Point, NC) using a 2.0-mm steel tip impounder at a controlled velocity (6.0 ± 0.2 m/sec) and impact depth (3.2 mm). Sham-injured animals underwent identical surgical procedures as the trauma group, but no impact was delivered. Mice with depressed skull fracture or visible hemorrhage were excluded from the study.

Induction of seizures using electroconvulsive shock

ECS was delivered using a commercially available device (Ugo Basile ECT Unit 57800; Harvard Apparatus, Holliston, MA), set to standard parameters (square wave mode for delivery of the pulse chain; pulse width of 0.4 msec; duration of 0.1 sec; frequency of 60 Hz), according to previously published methods (Altar et al., 2004; Ferraro et al., 1998, 2002). Briefly, each ear was dampened with skin prepping gel (Weaver and Company, Aurora, CO) and an electrode was secured to the pinna. The animals were allowed to move freely without anesthesia. The mouse was placed alone in a clear cage and the seizure was induced by application of electric current via the auricular electrodes. Control animals underwent handling and application of electrodes without delivery of ECS.

Quantification of the threshold current required for induction of seizures by electroconvulsive shock

The minimal current required to produce a seizure in the mouse is strain-dependent (Ferraro et al., 1998, 2002), but one has not been published for the CD1 strain used in these studies. To determine a threshold current for seizure onset in the CD1 strain, the animals were exposed to ECS of varying intensity. In the initial experiment, mice received only 1 shock each day with a maximum of 2 shocks per animal. After initial dose-finding experiments, a range of currents between 27 and 35 mA were evaluated in 1-mA increments. The response to ECS was videotaped and the presence of seizures determined by 2 separate observers. Subtle clinical signs of seizures including facial movement and forelimb clonus could not be reliably detected in this strain and were therefore excluded to minimize subjectivity in seizure assessment (Hunt et al., 2009). We defined seizure onset as forelimb clonus based on previously published methods (Ferraro et al., 1999; Frankel et al., 2001). We defined three responses on the continuum of the effects of ECS. They included (a) no seizure, and a return to normal activity of exploration and grooming; (b) hypoactivity, during which the mouse remained in a single location in

the cage in a crouched position with no limb movement; and (c) seizure. The scoring system used for seizure assessment was: 1, no seizure; 2, hypoactivity; 3, any limb extension (seizure). A hypoactive response to ECS was not scored as a seizure (Ferraro et al., 1999).

Treatment with small molecule inhibitor of proinflammatory cytokine upregulation

To determine whether suppression of the acute increase in proinflammatory cytokines after TBI would attenuate the subsequent increase in susceptibility to ECS-induced seizures, we used Minozac (Mzc), a small molecule, selective inhibitor of proinflammatory cytokine production by activated glia (Hu et al., 2007; Lloyd et al., 2008). We used the same dose and route of administration (5 mg/kg IP injection), and similar timing of administration (a total of 2 doses of Mzc, given at 3 h and 6 h following TBI), to those used in previous studies of TBI (Lloyd et al., 2008), and a two-hit model of seizures (Somera-Molina et al., 2007, 2009). Control animals were injected with an equal volume of saline (Sal) vehicle. This time window was selected based on the time course of the increase in proinflammatory cytokines we have previously reported (Lloyd et al., 2008), and to provide a clinically relevant delay in treatment after the primary insult.

Collection of brain tissue

At 8 or 14 days after TBI or sham procedure, the mice were anesthetized with isoflurane, and perfused via the left ventricle with 15 mL of chilled phosphate-buffered saline (PBS), followed by a second 15-mL perfusion with 4% paraformaldehyde in PBS. The brains were manually dissected from the calvarium with both cerebral hemispheres intact minus the cerebellum, and immersed in 4% paraformaldehyde overnight at 4°C. The brains were then cryopreserved in 20% sucrose in PBS overnight at 4°C before preparing 40-μm sections on a freezing microtome (HM 450; Microm, Walldorf, Germany).

Serial sections extending from bregma +0.5 mm to bregma −3.46 mm were prepared. This resulted in approximately 50 sections per brain. Every fifth section, separated by 200 μm, was mounted and used for analysis, yielding 10 sections per brain. For each of the 5 antibodies, 2 sections were used in sequence. The sequence of antibody processing was the same for each brain, and the two sections for each antibody were separated by at least 1 mm.

Immunohistochemical analyses of activated astrocytes and microglia, neuronal injury, and metallothionein expression

Immunohistochemical methods were used in frozen sections with minor modifications of published methods as we have previously described (Somera-Molina et al., 2009). Astrocyte activation was measured using antibodies to the glial-derived protein S100B (1:1000, mouse monoclonal; Millipore, Billerica, MA), and glial fibrillary acidic protein (GFAP; 1:6000, rabbit polyclonal; Dako Cytomation, Carpinteria, CA). Microglial activation was measured using antibody to Iba1 (1:1000, rabbit polyclonal; Wako Chemicals USA Inc., Richmond, VA). Expression of metallothionein (MT)-1 and MT-II was measured using commercially available antibody (1:500, mouse; Invitrogen, Carlsbad, CA). Neuronal injury was assessed using the neuronal nuclei marker NeuN (1:100, mouse monoclonal; Millipore). Negative control sections were incubated in normal serum or PBS in place of primary antibody. The sections were incubated with primary antibody or controls overnight at room temperature, washed, and then incubated for 1 h at room temperature with the appropriate biotinylated secondary antibody at 1:200 dilution. Immunohistochemical detection was performed using Vectastain Elite ABC immunodetection kits (Vector Laboratories, Burlingame CA), and diaminobenzidine substrate (DAB; Vector). All stained tissues except NeuN were counterstained with cresyl violet.

Image acquisition and quantification of immunoreactive cells

For each animal, for each antibody, two non-consecutive sections were immunostained, and one hemisphere per section was quantified. Hippocampal sections were examined under bright-field microscopy by two blinded observers (Nikon Eclipse E800; Nikon, Tokyo, Japan). For GFAP, S100b, Iba1, and MT staining, two consecutive regions of CA1 of the hippocampus were photographed at 40× magnification. Digitized images were quantified using ImageJ software (National Institutes of Health, Bethesda, MA). Immunolabeled cell bodies were considered positive counts, while cell processes were not counted. Total cell counts were normalized to the region (mm^2) counted. NeuN-immunolabeled sections were photographed at 10× magnification. The CA1 region of the hippocampus was qualitatively assessed for neuronal cell loss.

Hippocampal-linked task behavioral testing

The effect of TBI on hippocampal-dependent spatial learning was measured by testing performance in the Barnes maze (Barnes, 1979). Minor modifications were used of methods previously applied for evaluation of the rat following TBI (Fox et al., 1998; O'Connor et al., 2003). Animals were pre-trained on the Barnes maze four times per day for 4 days prior to TBI or sham procedure. After completion of training, the animals were randomized to experimental groups. A blinded observer assessed the post-procedure latencies to enter the maze escape box. Testing was performed by the same observer on days 7 and 14 of recovery at the same time of day for each session. Data were expressed as the latency time required to find the escape box in response to a stressful stimulus (examination light).

Statistical analysis

Values are expressed as mean ± SEM for each group. Tests for normality were performed for each data set. Parametric tests were used when the data were normal, and nonparametric tests were used if the data were not normal. One-way analysis of variance (ANOVA) (or the Kruskal-Wallis test for nonparametric analysis) was performed to compare three or more groups. Nonparametric seizure scores were compared between groups by the Kruskal-Wallis test. Bonferroni's multiple comparison procedure (or Dunn's procedure for nonparametric analysis) was used for *post-hoc* analysis. Determination of threshold current required to induce seizures

was measured by chi-square testing, with values dichotomized to seizures or no seizures. For Barnes maze testing, differences from baseline performance for each group were calculated by repeated measures ANOVA. Significance was defined as $p < 0.05$ for all tests. Prism 5.0 software (GraphPad Software, Inc., San Diego, CA) was used for statistical analyses.

Results

We first determined the threshold for seizure induction by ECS in the CD1 mouse strain (Fig. 1A). Stepwise increases in current intensity in naïve male mice identified 31 mA as the threshold for producing a clinical seizure in this strain (χ^2 $p < 0.0001$ for 30 mA versus 31 mA).

We hypothesized that TBI would increase susceptibility to seizures during recovery after TBI. To quantify changes in seizure susceptibility, we allowed the mice to recover for 7 days after TBI or sham procedure. We then administered ECS using the current (30 mA) identified in the previous experiment as below the threshold required to produce seizures in naive CD1 mice. We found a significant increase in seizure susceptibility (data are expressed as median seizure score ± interquartile range [IQR]) in mice which had undergone TBI (Fig. 1B). Treatment with Mzc at 3 and 6 h after the insult, to reduce the acute increase in proinflammatory cytokine upregulation produced by TBI (Lloyd et al., 2008), prevented this increased susceptibility. The seizure score for mice treated with Mzc after TBI was not significantly different from sham controls exposed to ECS.

We used immunohistochemical methods to measure changes in activated astrocytes and microglia in the CA1 region of the hippocampus following TBI, and to assess the effect of a second-hit with ECS-induced seizures on this response. To determine whether such activation contributed to increased susceptibility to seizures, we used Mzc to suppress glial activation, as we have described previously for TBI (Lloyd et al., 2008), and a two-hit kainic acid–induced seizure model (Somera-Molina et al., 2009). Mice underwent TBI or sham procedure, followed on day 7 of recovery by a single ECS using the minimal threshold current determined in the experiments above. Glial activation was assessed using GFAP (Fig. 2), and S100B (Fig. 3), after 1 further day of recovery from ECS (day 8 following TBI or sham procedure). When compared to sham controls (Fig. 2A), there was a significant increase in the density GFAP-immunoreactive (IR) astrocytes following TBI alone (Fig. 2C), and TBI combined with ECS (Fig. 2D). ECS alone did not lead to an increase in GFAP-IR astrocytes at 1 day recovery (Sham-ECS versus Sham-No ECS, not significant). Two-hit mice subjected to TBI prior to seizure induction on day 7 showed greater GFAP immunoreactivity than sham controls subjected to ECS alone (TBI-ECS versus Sham-ECS, $p < 0.001$ by ANOVA). Treatment with Mzc at 3 and 6 h following TBI attenuated this enhanced increase in GFAP-IR astrocyte density in mice subjected to the combination of TBI and ECS (Fig. 2E), but the difference in these values (Sham-ECS versus TBI-Mzc-ECS) did not reach statistical significance.

We found a similar pattern 24 h after the second hit with the astrocyte marker S100B (Fig. 3). Again, there were significant increases compared to sham controls in the density of S100B-IR cells following TBI alone (Fig. 3C), or TBI combined with

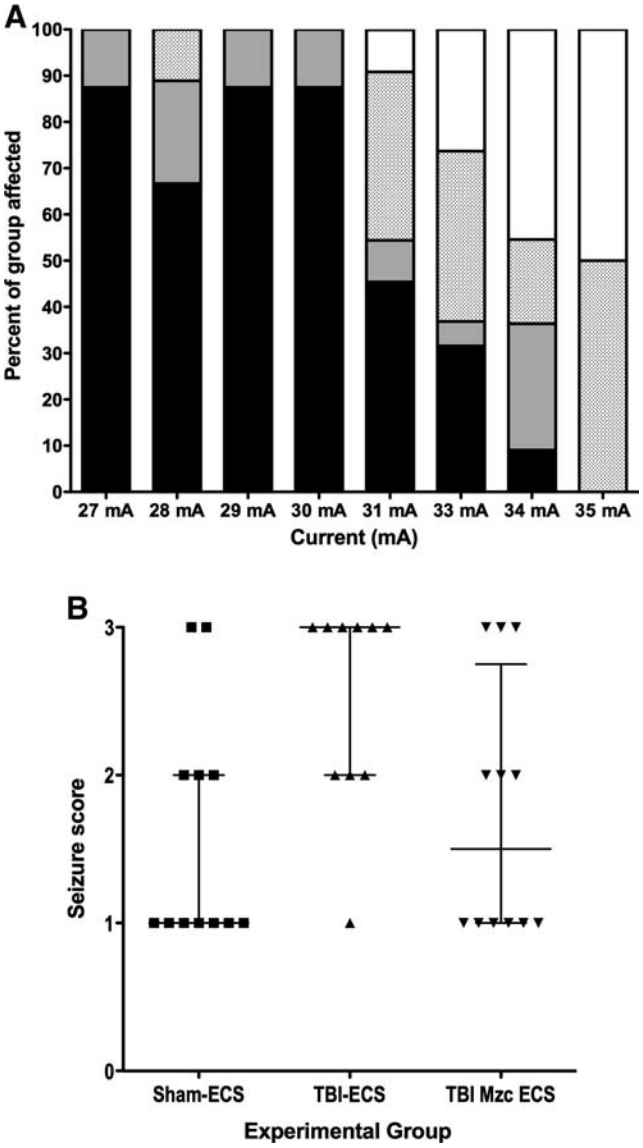

FIG. 1. (**A**) Stacked bar graph of responses to graded electroconvulsive shock (ECS) in naïve male CD1 mice. Mice were exposed to a single ECS in 1-mA increments from 27–35 mA ($n = 8$–19 per group). The response to ECS was videotaped and scored by separate observers as either no response (black), forelimb clonic seizure (grey), fore and hindlimb generalized tonic-clonic seizure (stippled), or death (white). The seizure threshold was determined to be 30 mA (χ^2 $p < 0.0001$ for 30 mA versus 31 mA). (**B**) Scatterplot of seizure scores (1, no seizure; 2, decreased activity; 3 forelimb or hindlimb clonic seizure) following 30-mA ECS-induced seizure on day 7 after TBI (TBI-ECS), TBI treated with the small molecule Minozac (TBI-Mzc-ECS), or sham procedure (Sham-ECS; bars indicate median seizure score ± interquartile range). The seizure score was significantly increased in mice subjected to TBI prior to ECS compared to sham controls (Sham-ECS versus TBI-ECS, $p < 0.05$ by Kruskal-Wallis test). This increase in seizure susceptibility after TBI was prevented by treatment at 3 and 6 h with Mzc (Sham-ECS versus TBI-Mzc-ECS, not significant; $n = 10$–12 per group; TBI, traumatic brain injury).

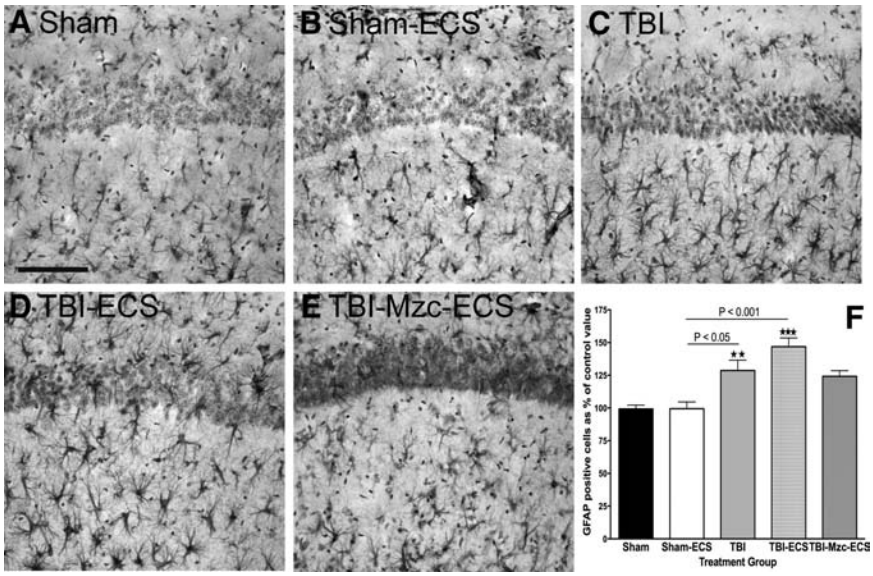

FIG. 2. Quantification of changes in the expression of the astrocyte marker glial fibrillary acidic protein (GFAP) in region CA1 of the hippocampus. All photomicrographs are of day 8 of recovery following sham procedure, traumatic brain injury (TBI), or TBI combined with a second-hit of electroconvulsive shock (ECS)-induced seizure on day 7. Representative photomicrographs of (**A**) sham controls on day 8, (**B**) sham mice administered ECS on day 7 (Sham-ECS) before sacrifice on day 8, (**C**) mice subject to TBI alone, (**D**) mice subjected to TBI combined with a second-hit of ECS (TBI-ECS) on day 7, and (**E**) TBI mice treated acutely with the small molecule Minozac (Mzc) to suppress proinflammatory cytokines (TBI-Mzc-ECS) before ECS on day 7 of recovery. Compared to sham controls, there were significant increases in GFAP following TBI alone (**C**, TBI), and TBI combined with ECS (**D**, TBI-ECS). Mice subjected to the two-hits (TBI-ECS) showed greater GFAP-immunoreactive (IR) cell density than ECS alone (Sham-ECS). Administration of Mzc at 3 and 6 h after TBI to suppress proinflammatory cytokines (**E**, TBI-Mzc-ECS) prevented the increase in GFAP produced by the second hit (Sham-ECS versus TBI-Mzc-ECS, not significant). GFAP-IR cells in digitized images were counted manually. (**F**) Values are expressed as a percentage of the cell count of the sham controls, and are expressed as mean ± standard error of the mean (** $p < 0.01$; *** $p < 0.001$ versus Sham-No ECS by analysis of variance; $n = 5$–6 per group). Positively stained cells are dark. Sections were counterstained with hematoxylin for contrast (scale bar = 100 μm).

ECS (Fig. 3D). This increase was again enhanced in the two-hit mice subjected to TBI-ECS compared to ECS alone (Fig. 3B) (TBI-ECS versus Sham-ECS, $p < 0.05$ by ANOVA). Treatment with Mzc prevented this enhanced increase (TBI-Mzc-ECS versus Sham-ECS, not significant) in S100B (Fig 3E).

We used the microglial marker Iba1 to measure differences in microglial responses under the same conditions (Fig. 4). Microglial responses to TBI or TBI combined with ECS were similar to those measured for GFAP and S100B. In contrast to GFAP and S100B, the increase in Iba1-IR cell density in the two-hit group was not prevented by treatment with Mzc (Sham versus TBI-Mzc-ECS, $p < 0.001$). Microglial activation was enhanced (Sham-ECS versus TBI-ECS, $p < 0.001$) in the two-hit group (Fig. 4D) compared to ECS alone (Fig. 4B). Treatment with Mzc did not prevent the enhanced response in the two-hit group (Fig. 4E).

Metallothioneins are upregulated in astrocytes following cerebral injury and are an important means of communication between injured neurons and astrocytes (Chung et al., 2004), which can be induced by proinflammatory cytokines (Quintana et al., 2007). As an initial step toward investigating the interactions between injured neurons and astrocytes before and after the second hit, we used immunohistochemical (IHC) methods to examine changes in the density of MTT-1 and MTT-II IR cells (Fig. 5). TBI alone, or ECS alone, did not produce significant increases in the density of MTT-IR cells compared to sham controls (Fig. 5A). However, the combination of TBI with ECS (Fig. 5B) resulted in a significant increase in MTT expression (Sham-ECS versus TBI-ECS, $p < 0.05$), which was prevented by treatment with Mzc after TBI (Fig. 5C).

These experiments indicated that the second hit of ECS-induced seizures after 1 week recovery from TBI resulted in enhanced astrocyte and microglial activation, and expression of MTT. To determine whether the prevention of this response by treatment with Mzc was sustained, we allowed mice to recover for a further 6 days after the second hit, and again quantified glial activation using the markers GFAP (Fig. 6A–D) and S100B (Fig. 6E–H) in CA1 14 days after the initial TBI or sham operation. Compared to sham controls exposed to ECS alone (Fig. 6A), the two-hit group of mice exposed to TBI and subsequent ECS (Fig. 6B) showed a significant increase in the density of GFAP-IR astrocytes (Sham-ECS versus TBI-ECS, $p < 0.001$). This enhanced response in the two-hit group was prevented by treatment with Mzc (Sham-ECS versus TBI-Mzc-ECS, not significant; Fig. 6C and D), consistent with the responses measured at the earlier time point 1 day after ECS-induced seizures. We found a similar pattern for S100B-IR cell density, including enhanced response in the two-hit group (Fig. 6F), and prevention of this response by Mzc (Fig. 6G and H). In contrast, there were no intergroup differences on day 14 in expression of Iba1 or MTT (data not shown).

We used IHC methods to quantify neuronal death (Somera-Molina et al., 2009). At 8- and 14-day recovery there were no

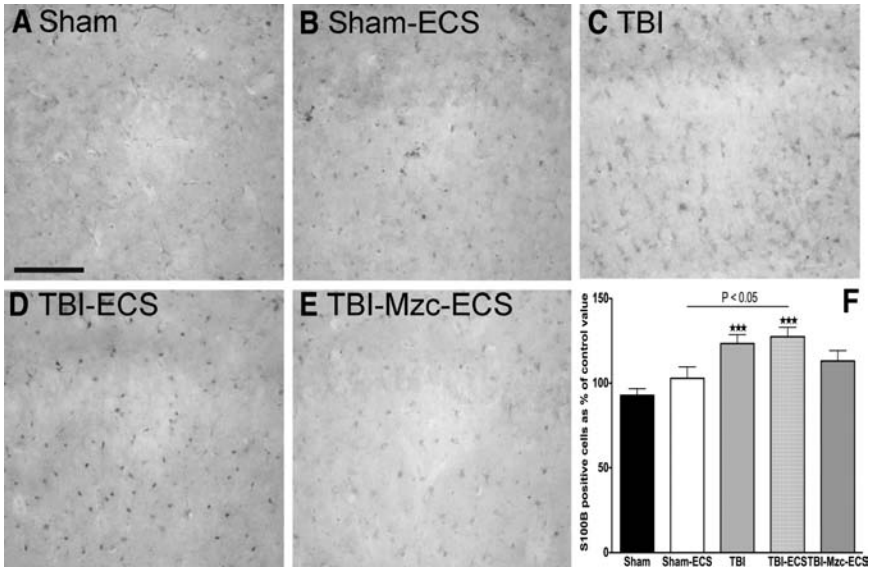

FIG. 3. Quantification of changes in the expression of the astrocyte marker S100B in region CA1 of the hippocampus. All photomicrographs are of day 8 recovery following sham procedure, traumatic brain injury (TBI), or TBI combined with a second-hit of electroconvulsive shock (ECS)-induced seizure on day 7. Representative photomicrographs of (**A**) sham controls (Sham), (**B**) sham mice administered ECS on day 7 (Sham-ECS) before sacrifice on day 8, (**C**) mice subjected to TBI alone (TBI), (**D**) mice subjected to TBI combined with a second-hit of ECS (TBI-ECS) on day 7, and (**E**) TBI mice treated acutely with the small molecule Minozac (Mzc) to suppress proinflammatory cytokines (TBI-Mzc-ECS) before ECS on day 7 of recovery. Compared to sham controls, there were significant increases in S100B-immunoreactive (IR) cell density following TBI alone (**C**, TBI), and TBI combined with ECS (**D**, TBI-ECS). Mice subjected to the two-hits (TBI-ECS) showed greater density of S100B-IR cells than ECS alone (Sham-ECS). Administration of Mzc at 3and 6 h after TBI to suppress proinflammatory cytokines (**E**, TBI-Mzc-ECS) prevented the increase in S100B produced by the second hit (Sham-ECS versus TBI-Mzc-ECS, not significant). S100B-IR cells in digitized images were counted manually. (**F**) Values are expressed as a percentage of the cell count of the sham controls, and are expressed as mean ± standard error of the mean; $^{***}p < 0.05$; versus Sham-No ECS by analysis of variance; $n = 5$–6 per group). Positively stained cells are dark (scale bar = 100 μm).

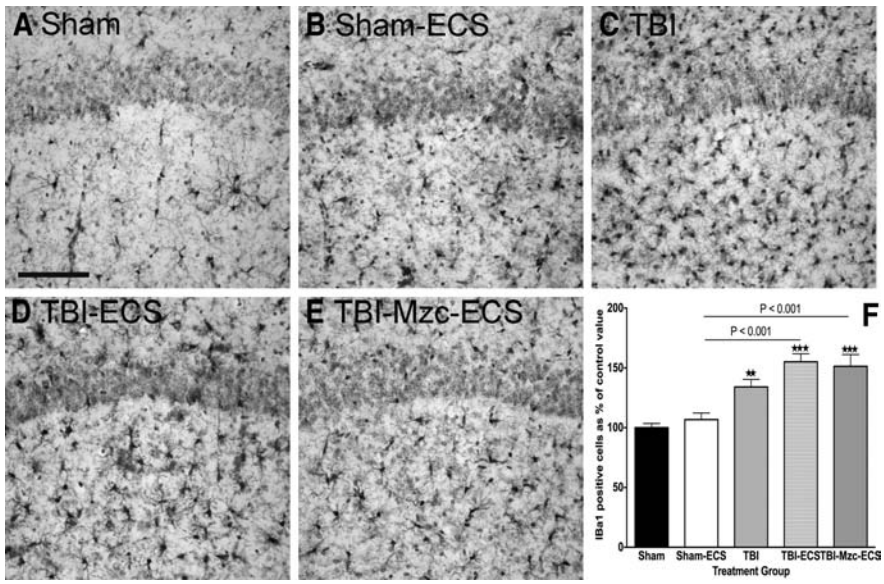

FIG. 4. Quantification of changes in the expression of the microglial marker Iba1 in region CA1 of the hippocampus. All photomicrographs are of day 8 recovery following sham procedure, traumatic brain injury (TBI), or TBI combined with a second-hit of electroconvulsive shock (ECS)-induced seizure on day 7. Representative photomicrographs of (**A**) sham controls on day 8, (**B**) sham mice administered ECS on day 7 (Sham-ECS) before sacrifice on day 8, (**C**) mice subjected to TBI alone, (**D**) mice subjected to TBI combined with a second-hit of ECS (TBI-ECS) on day 7, and (**E**) TBI mice treated with Minozac (Mzc) before ECS on day 7 of recovery (TBI-Mzc-ECS). Compared to sham controls, there were significant increases in the density of Iba1-immunoreactive (IR) cells following TBI alone (**C**, TBI), TBI combined with ECS (**D**, TBI-ECS) and two-hit mice treated with Mzc ($p <$, TBI-Mzc-ECS). Mice subjected to the two-hits (TBI-ECS) showed greater Iba1-IR cell density than ECS alone (Sham-ECS), which was not prevented by administration of Mzc at 3 and 6 h after TBI. Iba1-IR cells in digitized images were counted manually. (**F**) Values are expressed as a percentage of the cell count of the sham controls, and are expressed as mean ± standard error of the mean; $^{**}p < 0.01$; *** $p < 0.001$ versus Sham-No ECS by analysis of variance; $n = 5$–6 per group). Positively stained cells are dark. Sections were counterstained with hematoxylin for contrast (scale bar = 100 μm).

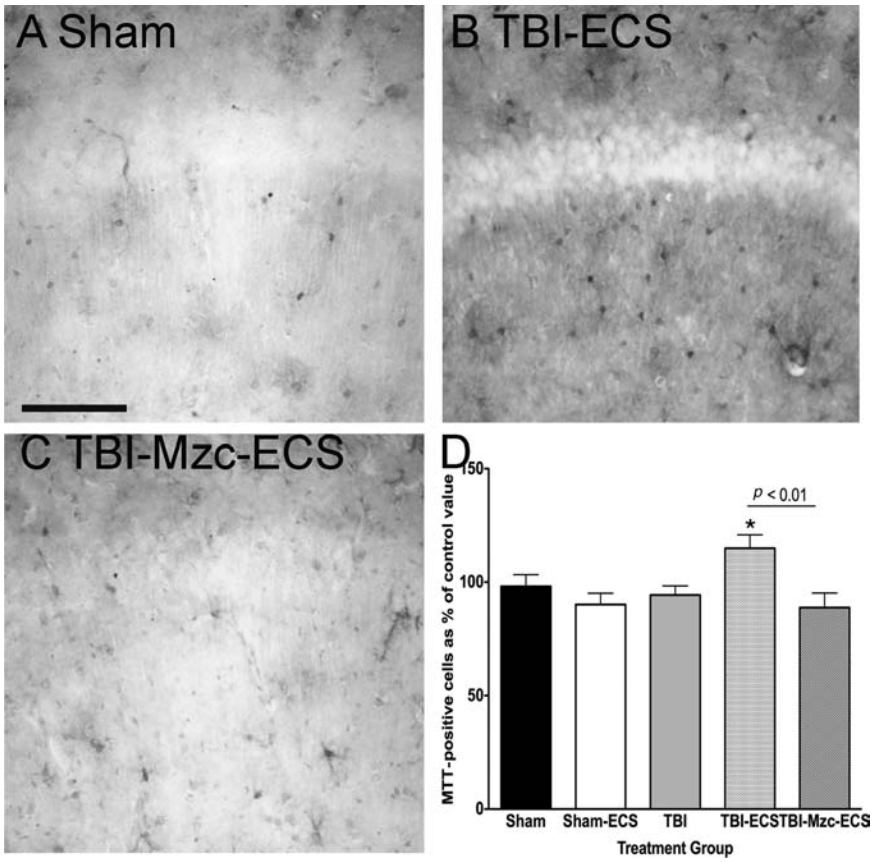

FIG. 5. Quantification of changes in the expression of metallothionein (MTT) in region CA1 of the hippocampus. All photomicrographs are of day 8 recovery following sham procedure, traumatic brain injury (TBI), or TBI combined with a second-hit of electroconvulsive shock (ECS)-induced seizure on day 7. Representative photomicrographs of (**A**) sham controls on day 8, (**B**) mice subjected to TBI combined with a second-hit of ECS (TBI-ECS) on day 7, and (**C**) TBI mice treated with Minozac (Mzc) before ECS on day 7 of recovery (TBI-Mzc-ECS). Compared to sham controls, there was a significant increase in the density of MTT-immunoreactive cells only in the two-hit group exposed to TBI combined with ECS (**B**). This increase was prevented by treatment with Mzc (**C**, TBI-Mzc-ECS). MTT-immunoreactive cells in digitized images were counted manually. (**D**) Values are expressed as a percentage of the cell count of the sham controls, and are expressed as mean ± standard error or the mean; $*p < 0.01$ versus Sham-No ECS by analysis of variance; $n = 56$ per group). Positively stained cells are dark (scale bar = 100 μm).

differences between groups in the density of NeuN-IR cells in region CA1 of the hippocampus (Fig. 7).

We used he performance in the Barnes maze (Barnes, 1979) as a measure of hippocampal-dependent behavior (Fig. 8). After pre-training (O'Connor et al., 2003) to establish baseline performance (latency to escape), mice were evaluated on day 7 of recovery after TBI or sham procedure. On day 8, mice were exposed to ECS to determine the effect of prior TBI on seizure susceptibility. On day 14 mice were again tested in the Barnes maze. In mice subjected to TBI, or TBI combined with ECS, there was significant impairment (increase in escape latency time) at day 14 of recovery. Notably, mice treated with Mzc immediately after TBI showed no impairment of function either on day 7 (prior to ECS), or on day 14, after the combination of TBI with ECS. Consistent with the enhanced glial activation observed in the two-hit (TBI-ECS) group, these mice also showed greater functional impairment than mice subjected to ECS alone (TBI-ECS versus Sham-ECS, $p < 0.01$ by ANOVA). Suppression of glial activation also prevented this enhanced neurocognitive impairment (TBI-Mzc-ECS versus Sham-ECS, not significant).

Discussion

There are three key findings of this study. First, a closed-skull midline TBI leads to a reduction in seizure threshold in the late phase of recovery. This is consistent with the reduction in seizure threshold reported after focal insults with controlled cortical impact (Statler et al., 2008) and weight drop (Golarai et al., 2001) in the rat. Second, the increase in seizure susceptibility is associated with greater glial activation with the second-hit of ECS, and suppression of the early cytokine response to TBI prevents this later increase in susceptibility. This finding suggests that enhanced glial activation contributes to the increase in seizure susceptibility seen after TBI, a mechanism we have previously identified as contributing to increased seizure susceptibility after early-life seizures (Somera-Molina et al., 2007, 2009). Last, the second hit with ECS after TBI also exacerbates the neurobehavioral impairment caused by TBI. This exaggerated functional impairment in the two-hit animals is also prevented by suppressing the glial response to TBI. Taken together, these findings implicate activation of glia both in the mechanisms of increased seizure

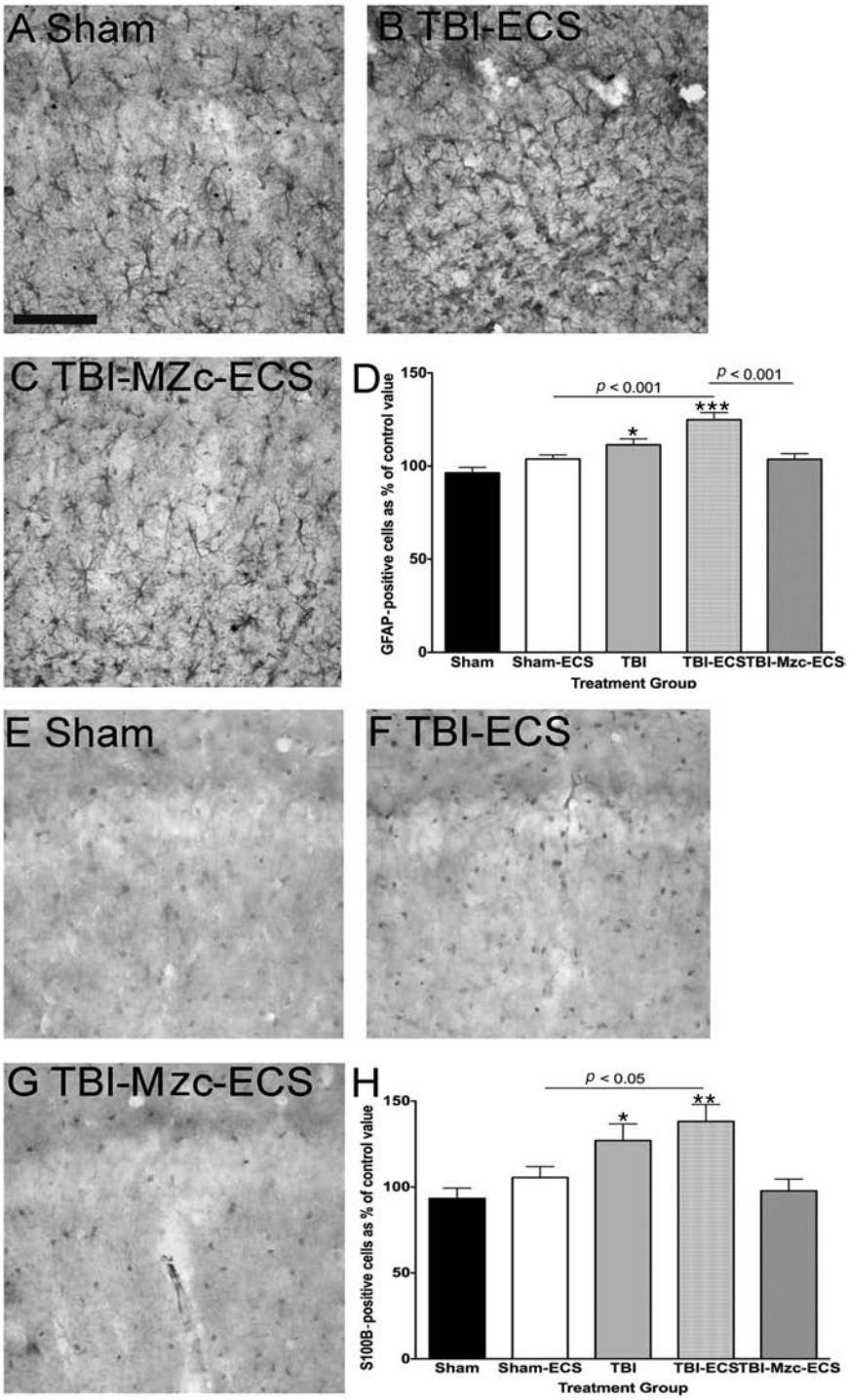

FIG. 6. Quantification of changes in the expression of glial fibrillary acidic protein (GFAP; **A**–**D**) and S100B (**E**–**H**) in region CA1 of the hippocampus. All photomicrographs are of day 14 recovery following sham procedure, traumatic brain injury (TBI), or TBI combined with a second-hit of electroconvulsive shock (ECS)-induced seizure on day 7. Compared to sham controls (**A**), there was a significant increase in the density of GFAP-immunoreactive (IR) astrocytes following TBI alone (not shown), and in the two-hit group exposed to TBI combined with ECS (**B**, TBI-ECS). Mice subjected to the two-hits showed increased GFAP-IR cells than ECS alone (Sham-ECS), and this response was prevented by treatment with Mzc (**C**, TBI-Mzc-ECS). A similar pattern was present for S100B (**E**–**G**), showing enhanced increase in the two-hit TBI-ECS group (**F**) compared to sham controls (**E**), and prevention of this response by Mzc treatment (**G**). GFAP- and S100B-IR cells in digitized images were counted manually. (**D** and **H**) Values in these graphs are expressed as percentages of the cell count of the sham controls, and are expressed as mean ± standard error of the mean; *$p < 0.05$; ** $p < 0.01$; *** $p < 0.001$ versus Sham-No ECS by analysis of variance; $n = 5$–6 per group). Positively stained cells are dark. Sections were counterstained with hematoxylin for contrast (scale bar = 100 μm).

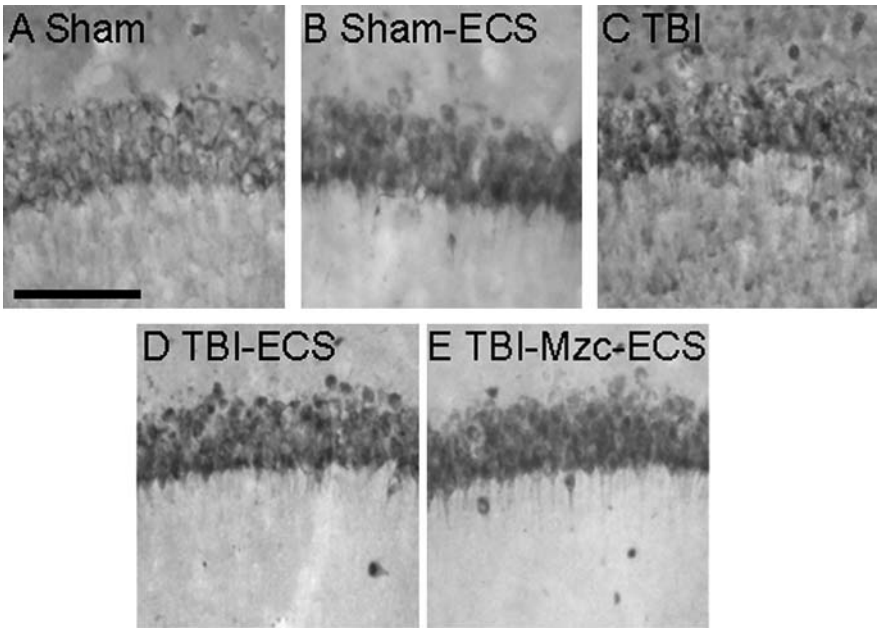

FIG. 7. Representative photomicrographs of NeuN-immunoreactive cells in region CA1 of the hippocampus. All photomicrographs are of day 14 recovery following sham procedure (**A**), sham combined with electroconvulsive shock on day 7 (**B**, Sham-ECS), traumatic brain injury (**C**, TBI), TBI combined with a second-hit of electroconvulsive shock (ECS)-induced seizure on day 7 (**D**, TBI-ECS) or two-hit animals treated with Minozac (**E**, TBI-Mzc-ECS). There were no significant intergroup differences in the density of NeuN-immunoreactive cells ($n = 5$–6 per group; scale bar = 100 μm).

susceptibility after TBI, and in the enhanced neurological injury seen after a second hit.

Multiple mechanisms have been identified in the processes leading to post-traumatic epilepsy (PTE), and many involve pathophysiological changes in the hippocampus (for review see D'Ambrosio and Perucca, 2004; Garga and Lowenstein, 2006). These include axonal sprouting (Golarai et al., 2001), impaired K^+ buffering by glia (D'Ambrosio et al., 1999), saturation of synaptic long-term potentiation of Schaffer collaterals (D'Ambrosio et al., 1998), hilar neuron loss (Lowenstein et al., 1992), and activation of hippocampal TrkB-ERK1/2-CREB/ELK-1 pathways (Hu et al., 2004). In part, advances in understanding have been limited by the lack of available animal models of late spontaneous seizures after TBI (Pitkanen and McIntosh, 2006). Evidence from studies of temporal lobe epilepsy (Buckmaster et al., 2002; Shibley and Smith, 2002) suggest that alterations in synaptic circuitry are a key mechanism of epileptogenesis. Hippocampal cell loss and mossy fiber sprouting produced by pharmacologically-induced seizures results in increased excitability in limbic pathways (Smith and Dudek, 2002). In slice preparations prepared 71 days after CCI in the mouse, mossy fiber sprouting was also detected (Hunt et al., 2009). Our data indicate an important role for activated glia in these complex processes.

Among the mechanisms of epileptogenesis, a number of lines of evidence suggest that Il-1β may play an important role that is directly relevant to TBI. Inhibition of IL-1β signaling by central overexpression of an IL-1β-receptor antagonist has a neuroprotective effect, and results in delayed proinflammatory cytokine induction and improved neurological recovery after TBI (Tehranian et al., 2002). After experimental brain trauma, IL-1β is upregulated within hours (Fassbender et al., 2000), and may act synergistically with TNF-α to increase injury (Chao et al., 1995). Using this TBI model, we have previously shown that proinflammatory cytokines including IL-1β and TNF-α are increased, and treatment with Mzc prevents this increase (Lloyd et al., 2008). Human and animal data identify a pivotal role for IL-1β (Balosso et al., 2008; Heida and Pittman, 2005; Ravizza et al., 2005, 2008), TNF-α (Galic et al., 2008), and persistent brain inflammation triggered by status epilepticus, in the mechanisms of epileptogenesis. The prevention of both increased seizure susceptibility and enhanced neurobehavioral impairment by suppression of cytokine elevation with Mzc in the present study are consistent with these observations.

We have previously shown that early-life seizures both increase susceptibility to seizures and result in enhanced neuronal injury with a second-hit of seizures in adulthood (Somera-Molina et al., 2007). The increase in seizure susceptibility in the two-hit animals subjected to seizures in early life and in adulthood was associated with greater astrocyte and microglial activation, and was prevented by treatment with a small-molecule inhibitor of proinflammatory cytokine upregulation (Somera-Molina et al., 2009). The increase in susceptibility to the second hit in the present model suggests a mechanism common to two-hit insults, in which the functional properties of astrocytes and microglia are altered during the latent period between insults.

As an initial step toward investigating the mechanisms by which glial responses to TBI may alter neuronal function, we measured changes in the zinc-binding proteins MT-1 and MT-II. Of the four MT mammalian isoforms, MT-I and MT-II are the most abundant in the brain, and are primarily expressed in astrocytes, serving to scavenge free radicals and maintain metal homeostasis, particularly zinc (for review, see Hidalgo

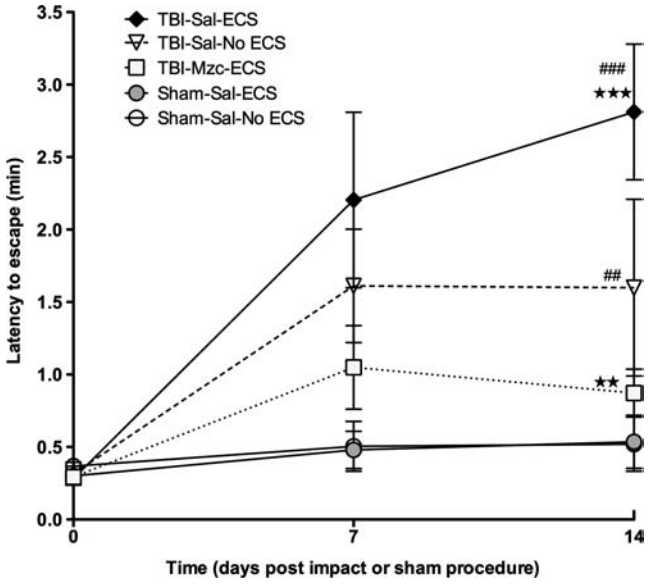

FIG. 8. Assessment of hippocampal-dependent behavior by latency to escape in the Barnes maze on days 7 (prior to electroconvulsive shock [ECS] on day 8) and 14 recovery after traumatic brain injury (TBI) or sham procedure (open circles, sham controls [Sham-Sal-No ECS]; gray circles, sham subjected to ECS [Sham-Sal-ECS]; triangles, TBI treated with saline [TBI-Sal-No ECS];diamonds, mice subjected to TBI combined with a second-hit of ECS on day 7 [TBI-Sal-ECS]; squares, TBI mice treated with Minozac before ECS on day 7 of recovery [TBI-Mzc-ECS]). Repeated-measures analysis of variance (ANOVA) with Bonferroni's post-test was used to determine differences of each group from baseline values. Differences between groups on day 14 of recovery were measured by ANOVA. On day 14, both the two-hit and TBI-alone groups were significantly impaired compared to their pre-injury performance. Treatment with Mzc after TBI prevented this in the two-hit group. Impairment was increased in the two-hit group on day 14 compared to TBI alone, and again this was prevented by Mzc treatment $^{**}p < 0.01$; $^{***}p < 0.001$ versus Sham-ECS by ANOVA; $^{\#\#}p < 0.01$; $^{\#\#\#}p < 0.001$ versus time point 0 by repeated-measures ANOVA; $n = 6$–7 per group).

et al., 2001). Mice lacking MT-I and MT-II show impaired recovery after neurologic insults including focal cortical injury (Trendelenburg et al., 2002). MT-I and MT-II expression by astrocytes is induced by neuronal injury (Chung et al., 2004). Following release from astrocytes, MT-1 and MT-II interact with LRP1 and LRP2 (megalin), which are low-density lipoprotein receptors (Ambjørn et al., 2007), leading to activation of both the PI3 kinase/Akt and MAPK pathways. MT-1 and MT-II are internalized by neurons, leading to axonal regeneration (Chung et al., 2008). Our data showing an increase in MTT following the second hit with ECS may reflect either greater neurological injury resulting in astrocyte release of MT-1 and MT-II, or an enhanced reparative response by activated astrocytes in the two-hit group.

We found evidence of cognitive impairment following TBI alone or TBI combined with ECS by testing with the Barnes maze. Although there was no neuronal death in CA1 in these groups, we quantified responses only in CA1, and it is possible that neuronal injury in other areas of the hippocampus was underestimated. The cognitive impairment in these groups suggests that neurological function is compromised. The prevention of these behavioral effects by attenuation of the glial responses to TBI suggests that activated glia contribute to neuronal dysfunction. This is consistent with our previous studies of the role of activated glia in the mechanisms causing increased susceptibility to neurological injury after early-life seizure (Somera-Molina et al., 2007), in which behavioral impairment and sustained glial activation occurred without neuronal death. Other studies using this TBI model have demonstrated hippocampal neuronal cell death using fluorescent detection of degenerating neurons with a shorter (1 day) recovery period (Laskowitz et al., 2007; Wang et al., 2007), in a different strain of mice. In addition, we used cell-counting methods of NeuN-immunoreactive neurons, a method that would not detect phagocytosed neurons, or NeuN-immunoreactive neurons that are dysfunctional. Last, the use of Mzc to modulate acute glial responses to the injury could be postulated to interfere with the phagocytic functions of glia during recovery. The improved performance in the Barnes maze test in the Mzc-treated group suggests that this may not be the case.

Microglial activation, as quantified by Iba1-immunoreactive cells, was enhanced in the two-hit animals compared to ECS alone. In contrast to the attenuation of the astrocyte responses to the second hit, this response was not prevented by treatment with Mzc. Our previous studies of a two-hit seizure model showed that Mzc does prevent enhanced microglial activation with the second hit (Somera-Molina et al., 2009), in which microglia may serve to amplify the neurological injury produced by the second insult. It is likely that different populations of microglia, secreting different neural effectors, are activated depending on the nature and severity of the insult (Lai and Todd, 2008; Lalancette-Hebert et al., 2007). Thus identification of the subpopulations of microglia expressing specific trophic factors and cytokines will be necessary in order to fully elucidate their role in the increased susceptibility to the second hit.

It is important to draw the distinction in the present studies between alterations in seizure susceptibility and models of PTE that produce spontaneous seizures. These latter models in the rat (D'Ambrosio et al., 2004; Kharatishvilli et al., 2006; Statler et al., 2009) and mouse (Hunt et al., 2009) produce a focal injury. It remains to be determined whether diffuse injury also results in spontaneous seizures, and if so by the same mechanisms. Such studies will require EEG monitoring and long-term outcomes as has been performed for the focal injury models. One potential benefit of using altered seizure susceptibility following TBI as a surrogate for epileptogenesis is the shorter recovery time required to conduct these studies. In the mouse pediatric PTE model, EEG monitoring was started 36 weeks post-injury (Statler et al., 2009). In the rat fluid percussion model of chronic spontaneous recurrent seizures (D'Ambrosio et al., 2005), the cumulative probability of detecting epileptiform discharges was greater than 80% after 4-week recovery. In contrast, the present study (7-day recovery), and a rat model of altered susceptibility (16–24 days; Statler et al., 2008), required only a short interval between insults.

The threshold for seizure induction in the CD1 mouse strain in these experiments is lower than that reported for the C57BL/6J strain, which is also commonly used in pre-clinical neurotrauma experiments. None of the male C57BL/6J mice

subjected to a single 35-mA electroshock responded with a maximal (tonic forelimb flexion, tonic hindlimb flexion, tonic hindlimb extension, and hindlimb clonus) seizure (Ferraro et al., 1998). Our study was not designed to evaluate the maximal seizure response. However, our finding that a current of this intensity produced a seizure or death in all sham CD1 mice, suggests that the seizure threshold in this strain is significantly lower than that of the C57BL/6J strain. This is consistent with the detailed study of the range of currents required to produce maximal seizure in other strains of mice, ranging from 24.4 mA in DBA 2J to 72.2 mA in C57BL/6J mice (Ferraro et al., 2002). While there may be some variation in the threshold due to differences in the electroshock stimulus (corneal or auricular electrode), use of a single- or repeated-seizure paradigm, and other factors, the majority of seizure susceptibility is genetically determined (Ferraro et al., 1998). The CD1 strain appears to be highly susceptible, in contrast to the C57BL/6J strain, which has the highest seizure threshold among the commonly used inbred mouse strains.

This study has a number of limitations. We investigated the effects of TBI on susceptibility to seizures, not the development of spontaneous seizures, which more precisely captures the evolution of PTE. EEG recordings were not performed, and it is possible that mice following TBI or TBI-ECS experienced electrographic seizures. The time period of recovery after the second hit and the interval between insults (1 week) was relatively short, in comparison to the duration (years), that may be required for the development of PTE. Last, the cell-counting method we used is less accurate than unbiased stereology.

These data provide further evidence that TBI lowers the threshold for seizures, and demonstrate that this response occurs after a closed-skull diffuse insult without neuropathological injury. The enhanced astrocyte and microglial activation associated with the second hit with ECS, and the prevention of the increase in seizure susceptibility by suppression of the early cytokine response with Mzc, together identify a mechanistic link between activated glia and PTE. These findings extend the mechanisms proposed for PTE, and identify selective modulation of activated glia as a potential therapeutic approach to attenuate the delayed neurological sequelae of TBI.

Acknowledgments

This work was supported by the Medical Research Junior Board Foundation (M.S.W.), the Lyndsey Whittingham Foundation (M.S.W.), and by NIH grants K12 HD052902 (C.V.), R01 NS056051 (D.M.W.), and KO8 NS044998 (M.S.W.).

Author Disclosure Statement

No competing financial interests exist.

References

Altar, C., Laeng, P., Jurata, L., Brockman, J., Lemire, A., Bullard, J., Bukhman, Y., Young, T., Charles, V., and Palfreyman, M. (2004). Electroconvulsive seizures regulate gene expression of distinct neurotrophic signaling pathways. J. Neurosci. 24, 2667–2677.

Ambjørn, M., Asmussen, J., Lindstam, M., Gotfryd, K., Jacobsen, C., Kiselyov, V., Moestrup, S., Penkowa, M., Bock, E., and Berezin, V. (2007). Metallothionein and a peptide modeled after metallothionein, EmtinB, induce neuronal differentiation and survival through binding to receptors of the low-density lipoprotein receptor family. J. Neurochem. 104, 21–37.

Balosso, S., Maroso, M., Sanchez-Alavez, M., Ravizza, T., Frasca, A., Bartfai, T., and Vezzani, A. (2008). A novel non-transcriptional pathway mediates the proconvulsive effects of interleukin-1β. Brain 131, 3256–3265.

Barnes, C. (1979). Memory deficits associated with senescence: A neurophysiological and behavioral study in the rat. J. Comp. Physiol. Psychol. 93, 74–104.

Buckmaster, P., Zhang, G., and Yamawaki, R. (2002). Axon sprouting in a model of temporal lobe epilepsy creates a predominantly excitatory feedback circuit. J. Neurosci. 22, 6650–6658.

Chao, C., Hu, S., Ehrlich, L., and Peterson, P. (1995). Interleukin-1 and tumor necrosis factor-alpha synergistically mediate neurotoxicity: involvement of nitric oxide and *N*-methyl-D-aspartate receptors. Brain Behav. Immun. 9, 355–365.

Chung, R., Adlard, P., Dittmann, J., Vickers, J., Chuah, M., and West, A. (2004). Neuron-glia communication: metallothionein expression is specifically up-regulated by astrocytes in response to neuronal injury. J. Neurochem. 88, 454–461.

Chung, R., Penkowa, M., Dittmann, J., King, C., Bartlett, C., Asmussen, J., Hidalgo, J., Carrasco, J., Leung, Y., Walker, A., Fung, S., Dunlop, S., Fitzgerald, M., Beazley, L., Chuah, M., Vickers, J., and West, A. (2008). Redefining the role of metallothionein within the injured brain. J. Biol. Chem. 283, 15349–15358.

D'Ambrosio, R., and Perucca, E. (2004). Epilepsy after head injury. Curr. Opin. Neurol. 17, 731–735.

D'Ambrosio, R., Fairbanks, J., Fender, J., Born, D., Doyle, D., and Miller, J. (2004). Post-traumatic epilepsy following fluid percussion injury in the rat. Brain 127, 304–314.

D'Ambrosio, R., Fender, J., Fairbanks, J., Simon, E., Born, D., Doyle, D., and Miller, J. (2005). Progression from frontal-parietal to mesial-temporal epilepsy after fluid percussion injury in the rat. Brain 128, 174–188.

D'Ambrosio, R., Maris, D., Grady, M., Winn, H., and Janigro, D. (1999). Impaired K(+) homeostasis and altered electrophysiological properties of post-traumatic hippocampal glia. J. Neurosci. 19, 8152–8162.

D'Ambrosio, R., Maris, D., Grady, M., Winn, H., and Janigro, D. (1998). Selective loss of hippocampal long-term potentiation, but not depression, following fluid percussion injury. Brain Res. 786, 64–79.

Fassbender, K., Schneider, S., Bertsch, T., Schlueter, D., Fatar, M., Ragoschke, A., Kuhl, S., Kischka, U., and Hennerici, M. (2000). Temporal profile of release of interleukin-1beta in neurotrauma. Neurosci. Lett. 284, 135–138.

Ferraro, T., Golden, G., Smith, G., DeMuth, D., Buono, R., and Berrettini, W. (2002). Mouse strain variation in maximal electroshock seizure threshold. Brain Res. 936, 82–86.

Ferraro, T., Golden, G., Smith, G., Jean, P.S., Schnork, N., Mulholland, N., Ballas, C., Schill, J., Buono, R., and Berrettini, W. (1999). Mapping loci for pentylenetetrazol-induced seizure susceptibility in mice. J. Neurosci. 19, 6733–6739.

Ferraro, T., Golden, G., Snyder, R., Laibinis, M., Smith, G., Buono, R., and Berrettini, W. (1998). Genetic influences on electrical seizure threshold. Brain Res. 813, 207–210.

Fox, G., Fan, L., Levasseur, R., and Fadden, A. (1998). Effect of traumatic brain injury on mouse spatial and non spatial learning in the Barnes circular maze. J. Neurotrauma 15, 1037–1046.

Frankel, W., Taylor, L., Beyer, B., Tempel, B., and White, H. (2001). Electroconvulsive thresholds of inbred mouse strains. Genomics 74, 306–316.

Galic, M., Riazi, K., Heida, J., Mouihate, A., Fournier, N., Spencer, S., Kalynchuk, L., Teskey, G., and Pittman, Q. (2008). Postnatal inflammation increases seizure susceptibility in adult rats. J. Neurosci. 28, 6904–6913.

Garga, N., and Lowenstein, D. (2006). Posttraumatic epilepsy: A major problem in desperate need of major advances. Epilepsy Currents 6, 1–5.

Golarai, G., Greenwood, A., Feeney, D., and Connor, J. (2001). Physiological and structural evidence for hippocampal involvement in persistent seizure susceptibility after traumatic brain injury. J. Neurosci. 21, 8523–8537.

Heida, J., and Pittman, Q. (2005). Causal links between brain cytokines and experimental febrile convulsions. Epilepsia 46, 1906–1913.

Hidalgo, J., Aschner, M., Zatta, P., and Vasak, M. (2001). Roles of the metallothionein family of proteins in the central nervous system. Brain Res. Bull. 55, 133–145.

Hu, B., Liu, C., Bramlett, H., Sick, T., Alonso, O., Chen, S., and Dietrich, W. (2004). Changes in TrkB-ERK1/2-CREB/Elk-1 pathways in hippocampal mossy fiber organization after traumatic brain injury. J. Cereb. Blood Flow Metab. 24, 934–943.

Hunt, R., Scheff, S., and Smith, B. (2009). Posttraumatic epilepsy after controlled cortical impact injury in mice. Exp. Neurol. 215, 243–252.

Hu, W., Ralay-Ranaivo, H., Roy, S., Behanna, H., Wing, L., Munoz, L., Van Eldik, L., and Watterson, D. (2007). Development of a novel therapeutic suppressor of brain proinflammatory cytokine up-regulation that attenuates synaptic dysfunction and behavioral deficits. Bioorgan. Med. Chem. Lett. 17, 414–418.

Kharatishvilli, L., Nissinen, J., McIntosh, T., and Pitkanen, A. (2006). A model of posttraumatic epilepsy produced by lateral fluid-percussion brain injury in the rat. Neuroscience 140, 685–697.

Lai, A., and Todd., K. (2008). Differential regulation of trophic and proinflammatory microglial effectors is dependent on severity of neuronal injury. Glia 56, 259–270.

Lalancette-Hebert, M., Gowing, G., Simard, A., Weng, Y.C., and Kriz, J. (2007). Selective ablation of proliferating microglial cells exacerbates ischemic injury in the brain. J. Neurosci. 27, 2596–2605.

Laskowitz, D., McKenna, S., Song, P., Wang, H., Durham, L., Yeung, N., Christensen, D., and Vitek, M. (2007). COG1410, a novel apolipoprotein E-based peptide, improves functional recovery in a murine model of traumatic brain injury. J. Neurotrauma 24, 1093–1107.

Lloyd, E., Somera-Molina, K., Nair, S., Van Eldik, L., Watterson, D., and Wainwright, M. (2008). Suppression of acute proinflammatory cytokine and chemokine upregulation by post-injury administration of a novel small molecule improves long-term neurologic outcome in a mouse model of traumatic brain injury. J. Neuroinflammation 5, 28.

Lowenstein, D., Thomas, M., Smith, D., and McIntosh, T. (1992). Selective vulnerability of dentate hilar neurons following traumatic brain injury: a potential mechanistic link between head trauma and disorders of the hippocampus. J. Neurosci. 12, 4846–4853.

O'Connor, C., Heath, D., Cermak, I., Nimmo, A., and Vink, R. (2003). Effects of daily versus weekly testing and pre-training on the assessment of neurologic impairment following diffuse traumatic brain injury in rats. J. Neurotrauma 20, 985–993.

Perry, V., Cunningham, C., and Holmes, C. (2007). Systemic infections and inflammation affect chronic neurodegeneration. Nat. Rev. Immunol. 7, 161–167.

Pitkanen, A., and McIntosh, T. (2006). Animal models of post-traumatic epilepsy. J. Neurotrauma 23, 241–261.

Quintana, A., Molinero, A., Florit, S., Manso, Y., Comes, G., Carrasco, J., Giralt, M., Borup, R., Nielsen, F., Campbell, I., Penkowa, M., and Hidalgo, J. (2007). Diverging mechanisms for TNF-alpha receptors in normal mouse brains and in functional recovery after injury: from gene to behavior. J. Neurosci. Res. 85, 2668–2685.

Ravizza, T., Gagliardi, B., Noe, F., Boer, K., Aronica, E., and Vezzani, A. (2008). Innate and adaptive immunity during epileptogenesis and spontaneous seizures: Evidence from experimental models and human temporal lobe epilepsy. Neurobiol. Dis. 29, 142–160.

Ravizza, T., Rizzi, M., Perego, C., Richichi, C., Veliskova, J., Moshe, S., De Simoni, M., and Vezzani, A. (2005). Inflammatory response and glia activation in developing rat hippocampus after status epilepticus. Epilepsia 46, S113–S117.

Rizzi, M., Perego, C., Aliprandi, M., Richichi, C., Ravizza, T., Colella, D., Veliskova, J., Moshe, S., De Simoni, M., and Vezzani, A. (2003). Glia activation and cytokine increase in rat hippocampus by kainic acid-induced status epilepticus during postnatal development. Neurobiol. Dis. 14, 494–503.

Schmidt, O., Heyde, C., Ertel, W., and Stahel, P. (2005). Closed head injury—an inflammatory disease? Brain Res. Rev. 48, 388–399.

Shibley, H., and Smith, B. (2002). Pilocarpine-induced status epilepticus results in mossy fiber sprouting and spontaneous seizures in C57BL/6 and CD-1 mice. Epilepsy Res. 49, 109–120.

Smith, B., and Dudek, F. (2002). Network interactions mediated by new excitatory connections between CA1 pyridamidal cells in rats with kainate-induced epilepsy. J. Neurophysiol. 87, 1655–1658.

Somera-Molina, K., Nair, S., Van Eldik, L., Watterson, D., and Wainwright, M. (2009). Enhanced microglial activation and proinflammatory cytokine upregulation are linked to increased susceptibility to seizures and neurologic injury in a 'two-hit' seizure model. Brain Res. 1282, 162–172.

Somera-Molina, K., Robin, B., Somera, C., Anderson, C., Stine, C., Koh, S., Behanna, H., Van Eldik, L., Watterson, D., and Wainwright, M. (2007). Glial activation links early-life seizures and long-term neurologic dysfunction: evidence using a small molecule inhibitor of pro-inflammatory cytokine up-regulation. Epilepsia 48, 1785–1800.

Sosin, D., Sniezek, J., and Thurman, D. (1996). Incidence of mild and moderate brain injury in the United States 1991. Brain Inj. 10, 47–54.

Statler, K., Scheerlinck, P., Pouliot, W., Hamilton, M., White, H., and Dudek, F. (2009). A potential model of pediatric post-traumatic epilepsy. Epilepsy Res. 86, 221–223.

Statler, K., Swank, S., Abildskov, T., Bigler, E., and White, H. (2008). Traumatic brain injury during development reduces minimal clonic seizure thresholds at maturity. Epilepsy Res. 80, 163–170.

Teasell, R., Bayona, N., Lippert, C., Villamere, J., and Hellings, C. (2007). Post-traumatic seizure disorder following acquired brain injury. Brain Inj. 21, 201–214.

Tehranian, R., Andell-Jonsson, S., Beni, S., Yatsiv, I., Shohami, E., Bartfai, T., Lundkvist, J., and Iverfeldt, K. (2002). Improved recovery and delayed cytokine induction after closed head injury in mice with central overexpression of the secreted form of the interleukin receptor antagonist. J. Neurotrauma 19, 939–951.

Temkin, N. (2001). Antiepileptogenesis and seizure prevention trials with antiepileptic drugs: meta-analysis of controlled trials. Epilepsia 42, 515–524.

Trendelenburg, G., Prass, K., Priller, J., Kapinya, K., Polley, A., Muselmann, C., Ruscher, K., Kannbley, U., Schmitt, A., Castell, S., Wiegand, F., Meisel, A., Rosenthal, A., and Dirnagl, U. (2002). Serial analysis of gene expression identifies metallothionein-II as major neuroprotective gene in mouse focal cerebral ischemia. J. Neurosci. 22, 5879–5888.

Van Eldik, L., and Wainwright, M.S. (2003). The Janus face of glial-derived S100B: beneficial and detrimental functions in the brain. Restorative Neurol. Neurosci. 21, 97–108.

Vezzani, A., and Baram, T. (2007). New roles for interleukin-1 beta in the mechanisms of epilepsy. Epilepsy Currents 7, 45–50.

Vezzani, A., and Granata, T. (2005). Brain inflammation in epilepsy: Experimental and clinical evidence. Epilepsia 46, 1724–1743.

Wainwright, M., Rossi, J., Schavocky, J., Crawford, S., Steinhorn, D., Velentza, A., Zasadzki, M., Shirinsky, V., Jia, Y., Haiech, J., Van Eldik, L., and Watterson, D. (2003). Protein kinase involved in lung injury susceptibility: evidence from enzyme isoform genetic knockout and in vivo. Proc. Natl. Acad. Sci. 100, 6233–6238.

Wang, H., Durham, L., Dawson, H., Song, P., Warner, D., Sullivan, P., Vitek, M., and Laskowitz, D. (2007). An apolipoprotein E-based therapeutic improves outcome and reduces Alzheimer's disease pathology following closed head injury: evidence of pharmacogenomic interaction. Neuroscience 144, 1324–1333.

Waxweiler, R., Thurman, D., Sniezek, J., Sosin, D., and O'Neil, J. (1995). Monitoring the impact of traumatic brain injury: a review and update. J. Neurotrauma 12, 509–516.

Weiss, G., Feeney, D., Caveness, W., Dillon, D., Kistler, J., Mohr, J., and Rish, D. (1983). Prognostic factors for the occurrence of post-traumatic epilepsy. Arch. Neurol. 40, 7–10.

Wyss-Coray, T. (2006). Inflammation in Alzheimer disease: driving force, bystander or beneficial response? Nature Med. 12, 1005–1015.

Address correspondence to:
Mark S. Wainwright, M.D., Ph.D.
Division of Neurology No. 51
Children's Memorial Hospital
2300 Children's Plaza
Chicago, IL 60614

E-mail: m-wainwright@northwestern.edu